

COUPLING IMPEDANCE STUDIES OF THE CURRENT TRANSFORMERS AT ALBA

T. F. Günzel, U. Iriso and A. Nosych, ALBA Synchrotron, Cerdanyola de Vallés, Spain

Abstract

ALBA is equipped with two different current transformers: FCT and DCCT. A third one, ICT, is now in design stage to be installed in 2019. A comparative study of different current transformers was carried out in order to characterize their contribution to longitudinal and transverse impedance. The gap in the vacuum chamber of the transformers was varied in order to study its effect on the heat deposited by the beam and on the resonance in the longitudinal impedance spectrum. Simulation results of ICT were compared to the experience with the existing current transformers in operation.

INTRODUCTION

The ALBA Storage Ring is currently equipped with two different Current Transformers to characterize the beam charge/intensity. The Fast Current Transformer (FCT) is used to measure the charge distribution or filling pattern, while the DC Current Transformer (DCCT) provides total (DC) beam intensity measurements with μA precision. In order to have an alternative beam current measurement, ALBA is going to install the new Integrating Current Transformer (ICT) in collaboration with Bergoz [1], who also provided the FCT and DCCT in the past.

The need for the design of new current transformer (ICT) bore the advantage of a comparative study of the already existing current transformers with the new one. The main goal of the study are to achieve an equivalent performance of the ICT in terms of collective effects to the existing devices (FCT and DCCT) and an understanding of the heat-up of the CTs.

The different devices (FCT, DCCT and ICT) will be analysed on the basis of resonant modes, longitudinal and transverse impedance and their associated loss/kick factors computed by GdfidL [2]. A couple of different geometry and material options for each device will be discussed. Most of simulation work is straightforward except that of the coil, whose consideration was forcefully simplified.

ANALYSIS TOOLS

The longitudinal impedance spectra analysis was combined with the eigenmodes computed by GdfidL. T- and F-domain computations are actually not equivalent but both provide a complementary image of the full picture. The resonances, in particular their frequencies, found in the impedance spectra are rather precise, and show a very good picture in terms of modes whereas the eigenmode computations depend on a couple of external parameters difficult to optimise. The eigenmode solver, however, generates more modes than resonances exist, so some of them are just propagating (and therefore not real), but it helps in recognizing

small resonances. Moreover, it provides a shunt impedance R_s whereas the height of resonances in impedance spectra depend on the length of the trailer of the witness particle.

The shunt impedance can be directly compared to the threshold of longitudinal coupled bunch instabilities (LCBI): see next sub-section. The shunt impedance value here is only based on the dissipative quality factor, which does not consider losses (called radiative losses) generated by a slipping of the resonance' field out of its trapping location. In general (as long as the shunt impedance does not exceed the threshold) the dissipative shunt impedance is sufficient as adding radiative losses will only reduce it more¹. Both data are shown in an overlay of the eigenmode's shunt impedance (in red) on the real's part impedance spectrum (in blue) in logarithmic scale in order to cover a large dynamic range.

The Threshold Criterion

It essentially requires the sampling of the impedance $Z_l(\omega_m)$ at the resonance peak $\omega_m = (Mj\omega_0 + m\omega_0)$ only once² and at $-(Mj\omega_0 - m\omega_0)$ close to the mirror peak $Z_l(-\omega_m)$. Its negative contribution can partially cancel out the positive one, but it usually does not happen for narrow peaks (ω_0 is the angular rev. frequency, $M = 448$ the harmonic number, j any integer and an appropriate $0 \leq m \leq M - 1$). Neglecting the negative contribution altogether makes the criterion stricter, but much simpler. As long as resonances stay below the threshold of this criterion LCBI's cannot be excited. The suchlike sampled impedance is compared to the threshold impedance:

$$R_s^{\text{threshold}} = \frac{\omega_s \omega_r \sigma_\tau^2 T_0 (E/e)}{\tau I \alpha \exp(-(\omega_r \sigma_\tau)^2) I_1((\omega_r \sigma_\tau)^2)} \quad (1)$$

where I_1 is the 1st modified Bessel function, ω_s and ω_r stand resp. for the angular synchrotron and resonance frequency, σ_τ for bunch length, $T_0 = 2\pi/\omega_0$, τ for long. damping time and E for the beam energy, α for the momentum compaction factor and I the multibunch current (here 0.4A). Normally the assumption $I_1(x) \approx 0.5x$ for $x \ll 1$ is made, which is no longer true for $\omega_r/(2\pi) \approx 5 - 7\text{GHz}$.

CURRENT TRANSFORMERS

All the CTs at ALBA have a gap in the beampipe to allow the magnetic coil to see the image currents (see Fig. 1). Its geometry is characterized by the gap length and its height — also called “nose” — which allows to modulate its capacitance. In the simulations, particular attention is paid to the

¹ In the meantime GdfidL provides a combination of both, but disposing of both distinguished information was preferred.

² multiple hits are actually possible with low Q, but then R_s will be minor.

Content from this work may be used under the terms of the CC BY 3.0 licence (© 2019). Any distribution of this work must maintain attribution to the author(s), title of the work, publisher, and DOI

gap, which for both the FCT and DCCT are 1 mm width and 4 mm height (not including the 0.5 mm of the beam shield).

Both devices are rather similar, but some differences exist: the DCCT is 80mm longer, and the position of the ceramics wrt the beam pipe gap is upstream for the FCT, but downstream for the DCCT. Furthermore, the FCT's ceramic which isolates the coil from the device's interior is separated from the beam pipe's gap by a vertical support disk.

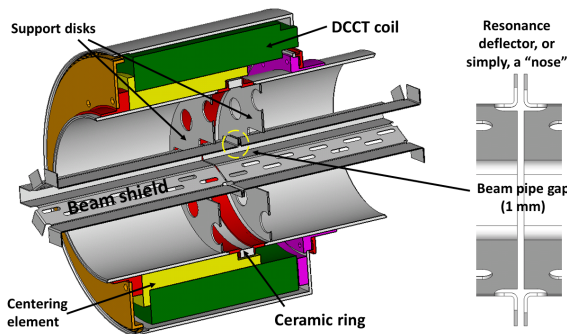


Figure 1: DCCT device cross-section and its 1 mm pipe gap zoom-in.

FCT and DCCT without Space for the Coil

The longitudinal spectra are characterized by an important resonance at low frequency generated by the gap in the beam shield (Fig. 2,3) which is at higher frequency for the FCT than for the DCCT probably due to the different support disk positions confining the different space close to the beam pipe gap.

Only a marginal effect of the lossy character of the ceramics $\tan(\delta) = 4 \cdot 10^{-4}$ on the power distributions was found. Therefore in the following the lossy character of the ceramics is neglected.

FCT and DCCT with Space for the Coil

Actually, a description of the coil was not possible because of its unknown parameters (for reasons of commercial confidentiality). Therefore simply the geometry of the empty cavity ($\mu = 1$) was simulated. In the simulation the cavity is in direct contact with the ceramics although in reality (one for the FCT; five for the DCCT) thin Al-sheets separate ceramics and cavity. These 5 layers of Al-sheets are there to keep the capacitance of the DCCT within the manufacturer ranges: between 10 and 220 nF. The numerous Al-sheets do not allow the electrical and magnetic field's AC part to penetrate beyond. Therefore the space (and what it might contain) beyond the ceramics of DCCT should not have a sensible effect on the impedance, whereas in the FCT case it is still possible due to the weaker shielding.

In the following, an unshielded cavity beyond the ceramics will be assumed for both CTs as a worst case estimation. Such a cavity will catch part of the energy of beam and store it for a limited time until it is dissipated in the walls and/or taken up by the coil. The caught energy is reflected in additional resonant peaks at low frequency in the impedance

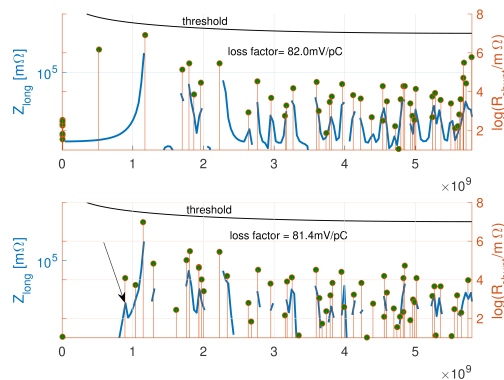


Figure 2: FCT w/o & with coil cavity: $Re(Z_l)$ & modes' R_s , due to the cavity an additional peak @ low frequency marked by an arrow.

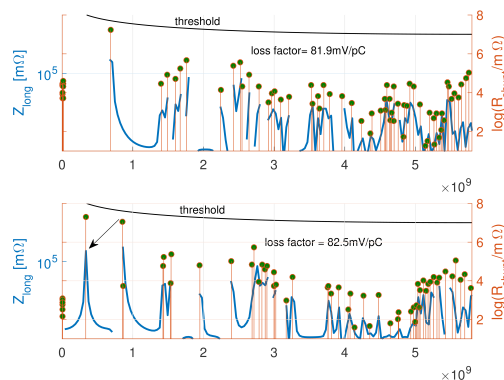


Figure 3: DCCT w/o & with coil cavity: $Re(Z_l)$ & modes' R_s , due to the cavity an additional peak @ low frequency marked by an arrow.

spectra (Fig. 2,3). The coil will slightly change the energy content in this cavity and therefore have an influence on the resonances. Nevertheless, these details are not of major importance as the loss factor is almost unchanged with or without additional cavity.

Due to the vertical support disk between gap and ceramic the effect of the cavity is substantially suppressed in the FCT. Removing the support disk, however, enhances the resonance significantly.

ICT

The basics of the ICT geometry are similar to the ones in Fig. 1, but the main difference is that the ceramic ring is not shifted along the beam direction with respect to the gap. In order to optimize the ICT design, a parametrical study (w/o consideration of the coil nor its cavity) showed that larger noses and smaller gaps reduce the long. impedance (Fig. 4). The goal of reaching a comparable loss factor to those of the FCT/DCCT was achieved with a nose of 3.5mm (+1mm beam shield) (Fig. 6).

Eventually the cavity beyond the ceramics was considered ($\mu = 1$) and alternatively filled up with material $\mu = 10$ or $\mu = 100$ to know more about the effect of the coil it contains. The resonance structure changes, in particular the lowest resonance frequency decreases with increasing μ (Fig. 5) —

therefore the ICT design will be modified [4] — but the loss factor remains more or less the same (the agreement between GdfidL’s T- and F-domain is actually less good for $\mu \gg 1$ since many eigenmodes with less accuracy are computed). We conclude that an exact characterization of the coil will not change significantly the already known loss factor.

Possible heat sources have been searched for. The power losses are above all found in the nose of the devices (Fig. 7). It amounts to a bit more than 3W for the FCT wrt DCCT @0.2A. Possible heat deposition in the ceramics due to infrared radiation from the nose is suspected. A temperature distribution will be computed in the near future. The longitudinal impedance’ real part of a ceramics with a $\tan(\delta) = 4 \cdot 10^{-4}$ turned out to be $0.45 \text{ m}\Omega \cdot f \text{ [GHz]}$ [3], which is rather small.

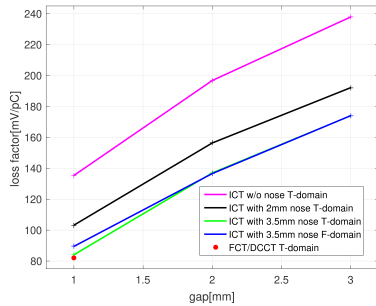


Figure 4: Loss factors (cut off @5.8GHz) for different gaps and noses of the ICT compared to FCT/DCCT (red dot)

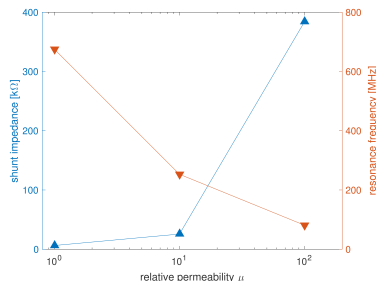


Figure 5: Resonant frequency & shunt as a function of μ

TRANSVERSE IMPEDANCE

For the three devices the dipolar transverse impedance was computed. The numbers can be found in Tab. 1. All the CTs are installed almost consecutively, so the β -function can be considered equal. Note that the ICT design provides similar impedance values as the FCT and DCCT.

Table 1: β_V -Weighted Eff. Trans. Impedance (in $\text{k}\Omega$)

element	$\beta_V[\text{m}]$	$\beta_H[\text{m}]$	Z_{eff}^V	Z_{eff}^H
FCT	5.2	8.7	1.32	1.17
DCCT	5.2	8.7	1.44	1.18
ICT	5.2	8.7	1.31	1.14

CONCLUSION

Similar longitudinal impedance and thereby loss factors of the FCT, DCCT and ICT were found which amount to

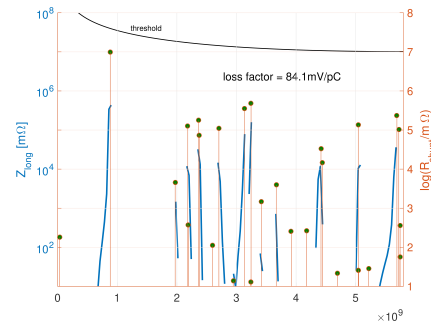


Figure 6: ICT w/o cavity: $Re(Z_l)$ & the eigenmodes’ R_s

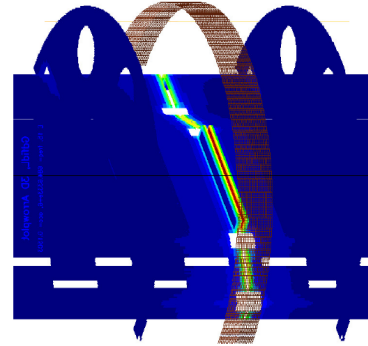


Figure 7: Typical magnetical field map in the ICT.

$81 - 84 \frac{\text{mV}}{\text{pC}}$ @4.6mm bunch length corresponding to powers of 6.6 – 6.84 W at 0.2 A in a bunch train of 440/448 bunches filled. It is mainly determined by a strong resonance at rather low frequency 600 – 1200MHz. The height of the resonances always stays below the instability threshold of LCBI’s (further inclusion of the Q-values associated with the radiation loss was not necessary to demonstrate this). A parametrical study showed that small gap and a large nose decrease the impedance and thereby the loss factor of the ICT. Attributing the coil with permeability larger than 1 changes the resonance structure at low frequency, but leaves the loss factor unchanged. The ICT will be installed in September, and further details about its performance will be shown in Ref. [4].

REFERENCES

- [1] <http://www.bergoz.com>
- [2] W. Bruns, <http://www.gdfidl.de>
- [3] B. Zotter, “Longitudinal instabilities of charged particle beams inside cylindrical walls of finite thickness”, *Part. Acc.*, vol. 1, pp. 311–326, 1970.
- [4] A. Nosych, T. Günzel and U. Irso, “Design and Performance of the ICT for ALBA”, to be presented at IBIC’19, Malmö, Sweden, September 2019.